SEISMIC BEHAVIOR OF RC BEAMS WITH CURTAILED SECOND LAYER LONGITUDINAL REINFORCEMENT

R. Rinaldi(1), T. Obara(2), S. Kono (3), D. Mukai (4), Y. Murata (5), F. Iihoshi (6)

(1) Graduate Student, Tokyo Institute of Technology, rickyrinaldi04@gmail.com
(2) Assist. Prof., Tokyo Institute of Technology, obara.t.ac@m.titech.ac.jp
(3) Prof., Tokyo Institute of Technology, kono.s.ae@m.titech.ac.jp
(4) Assoc. Prof., University of Wyoming, (Visiting Assoc. Prof., Tokyo Institute of Technology), dmukai@uwyo.edu
(5) Neturen Co., Ltd., y-murata@k-neturen.co.jp
(6) Neturen Co., Ltd., f-iihoshi@k-neturen.co.jp

Abstract

High-strength steel reinforcement provides many benefits to reinforced concrete (RC) constructions such as reducing cost and improving workability. In Japan, steel reinforcement with nominal yield strength up to 1275 MPa is commercially available, enabling more efficient use of shear reinforcement. However, reducing the amount of shear reinforcement may lead to bond failure of longitudinal bars. RC members with curtailed longitudinal bars are particularly prone to the bond failure due to the higher bond stress demand on the second layer bar. A method was proposed on the 1999 AIJ Guidelines to predict the load-carrying capacity for bond splitting failure in RC members with continuous longitudinal reinforcement. However, the existing method is not able to well predict the failure mode of beams with curtailed second layer reinforcement.

This paper examines the bond performance of six reinforced concrete beams with curtailed second layer longitudinal reinforcement confined by 1275MPa class shear reinforcement. The variables were shear reinforcement ratio, concrete strength, curtailment length, and amount of second layer longitudinal bars. The 1999 AIJ Guidelines equation was used to evaluate the bond strength of second layer bars. The test results showed that the increase of shear reinforcement increased bond strength of second layer longitudinal bar significantly. The ratio of experimental to calculated bond strength increased from 0.97 to 1.32 by doubling the amount of shear reinforcement. The failure mode of three specimens was bond and that of the remaining three specimens was a mixture of shear and bond failure. The results from this study are useful to evaluate the failure mode of RC members with curtailed second layer longitudinal bars confined by high strength shear reinforcement.

Keywords: high strength reinforcement; bond failure; curtailed bar; failure mode; crack evaluation

1. Introduction

Reinforced concrete members with insufficient steel confinement are vulnerable to bond failure. Curtailed longitudinal reinforcement is particularly prone to bond failure due to the limited bond length. Various design methods [1,2] have been developed for RC members to avoid bond failure. The 1999 AIJ Guidelines [1] equations had been proven adequate in estimating the load carrying capacity of beams confined with 1275MPa class high strength reinforcement [5,6]. However, it is still unclear how to determine the failure mode using the current design method. Bond strength is an important factor in determining load carrying capacity and failure mode of RC beams. For years, the bond strength of second layer bars has been estimated by assuming the side-splitting bond failure, as shown in Fig. 1 (a). Pull-out tests by Nishimura and Kawazu [3][4] revealed that the bond strength of multiple layered bars needs additional evaluation based on lateral splitting failure, as shown in Fig. 1 (b). However, test data available to evaluate such bond failure on RC beams with high strength shear reinforcement is still limited.

The research described herein investigates the failure mode of RC beams with curtailed second layer reinforcement confined by high strength shear reinforcement. The specimens were composed of six RC beams with various configurations of curtailed bars and shear reinforcement. Maximum bond stress and load carrying capacity were evaluated according to the 1999 AIJ Guidelines [1] and Nishimura and Kawazu [3][4].

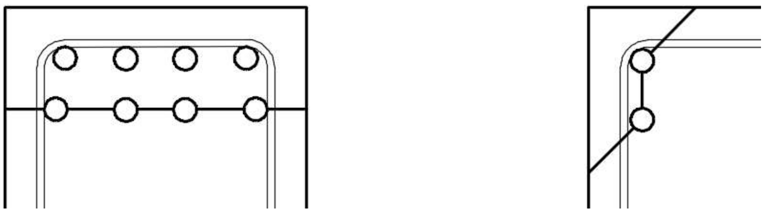

(a) Side Split Mode [1][2]　　(b) Lateral Split Mode [3]

Fig. 1 – Bond Split Failure Modes

2. Experimental Setup

The test variables and reinforcement properties are listed in Table 1. All specimens had U7.1 (1275MPa Class nominal yield strength) shear reinforcement and two layers of longitudinal bars, as shown in Fig 2. N-5-3 was a benchmark specimen, N-5-2 had fewer second layer bars, and N-5-4 had greater number of second layer bars. H-5-3 had higher concrete strength of 56.6 MPa. H-ld was identical to H-5-3 except for its longer curtailment length of the second layer bars. H-pw had the highest shear reinforcement ratio of 0.55%. The curtailment length of the second layer bars L_D was designed using Eq. (1)[1] except for H-ld whose curtailment length was designed longer than H-5-3. The nominal yield strength in Eq. (1) was assumed to be 345 MPa to represent ordinary strength reinforcement in common practice. All specimens were designed to fail in bond based on the 1999 AIJ Guidelines [1].

Lateral load was applied by two horizontal jacks, as shown in Fig. 3. The upper concrete block was kept parallel with the lower concrete block throughout the loading. Two restrainers were attached to resist the out-of-plane deformation. Loading was controlled by drift angle (R), which was the ratio of lateral displacement and clear span (L = 2000 mm). Loading protocol consisted of two cycles of R=±0.125%, ±0.25%, ±0.50%, ±0.75%, ±1.00%, ±1.50%, ±2.00%, ±3.00 and ±4.00%. Loading was terminated when the load carrying capacity dropped for more than 20% of its maximum load.

$$L_D = \frac{\sigma_s A_s}{\tau_{bu2}\psi} + d \qquad (1)$$

A_s : nominal bar section area (mm^2)
ψ : bar circumferential length (mm)
d : beam effective depth (mm)
σ_s : nominal yield strength (345 MPa)
τ_{bu2} : bond strength of the second layer bar (MPa) [1]

Table 1 – Specimen Properties

No.		1	2	3	4	5	6
Specimen		**N-5-2**	**N-5-3**	**N-5-4**	**H-5-3**	**H-ld**	**H-pw**
Concrete	Compressive Strength f_c (MPa)	25.9	25.6	28.9	56.6	59.4	60.7
Longitudinal Reinforcement	Configuration	5+2 D22 (SD590)	5+3 D22 (SD590)	5+4 D22 (SD590)	5+3 D22 (SD685)		
	Yield Strength f_y (MPa)	645			716		
	Young's Modulus E_s (GPa)	190			197		
	Curtailment Length L_D (mm)	650	790	940	750	830	750
Shear Reinforcement	Configuration	4-U7.1 @100	4-U7.1 @100	4-U7.1 @100	3-U7.1 @125	3-U7.1 @125	3-U7.1 @62.5
	Yield Strength f_y (MPa)	1404					
	Ratio ρ_w (%)	0.46			0.27		0.55
Role		Less curtailed bars	Benchmark	More curtailed bars	Higher f_c	Longer L_D	Higher ρ_w

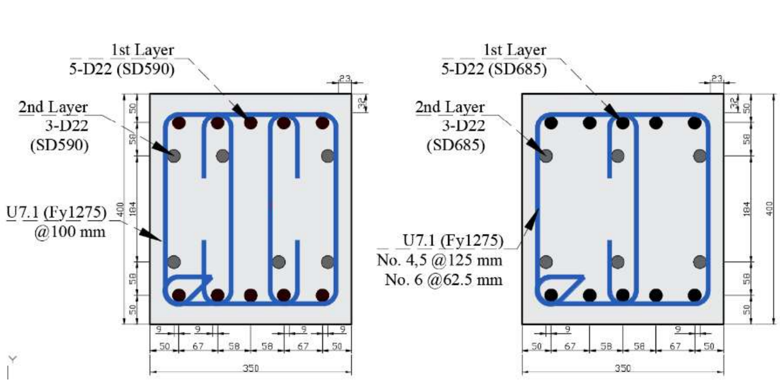

(a) No. 2 (b) No. 4, 5, and 6

Fig. 2 – Beam Cross Section (Unit in mm)

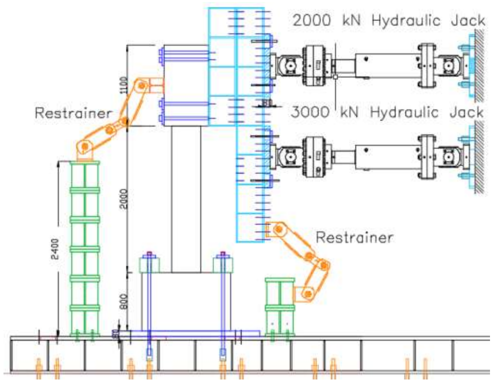

Fig. 3 – Loading System

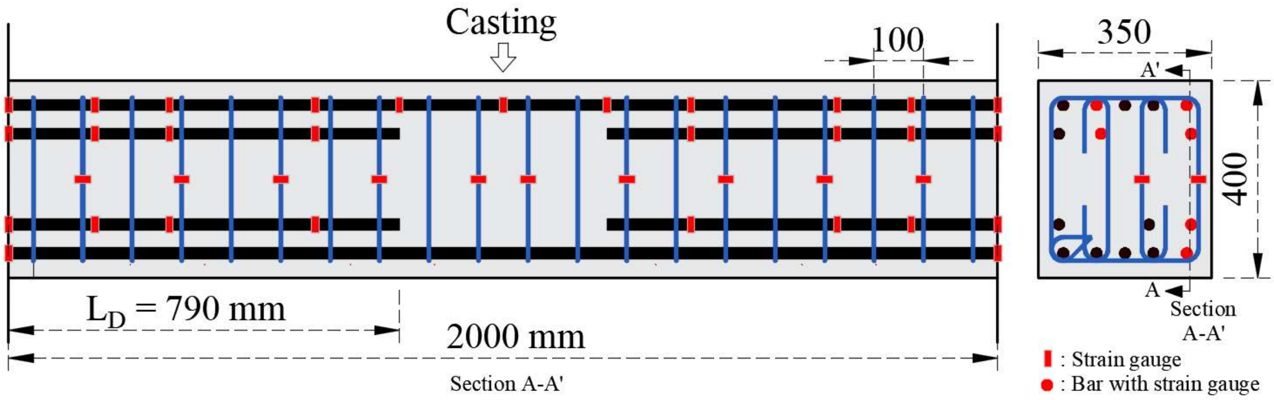

Fig. 4 – Strain Gauges Location for N-5-3

3. Bond Strength of Longitudinal Bars

Strain distribution of longitudinal bars for N-5-3 is shown in Fig. 5. The strain data is plotted for every peak of positive load cycle from R=+0.125% until +3.00%. No longitudinal bar reached the yield strain throughout the loading. Bond stress was computed using strain gauge reading at two locations; the end of effective depth region (d) and at curtailment point as highlighted by broken lines in Fig. 5.

The maximum bond stress of the second layer bar τ_{b2} was compared with the 1999 AIJ Guidelines equations for bond strength τ_{bu2} as shown in Fig. 6 (a). Results from previous experiments on curtailed second layer bars [5,6] are also presented. The maximum bond stress increased significantly by doubling the amount of shear reinforcement as seen from H-5-3 and H-pw. The ratio τ_{b2}/τ_{bu2} for H-5-3 and H-pw were 0.97 and 1.32, respectively. The maximum bond stress τ_{b2} of most specimens were higher than the calculated value τ_{bu2}, except for N-5-2, N-5-3, and N-5-4. The lowest τ_{b2}/τ_{bu2} was 0.42 for specimen N-5-2.

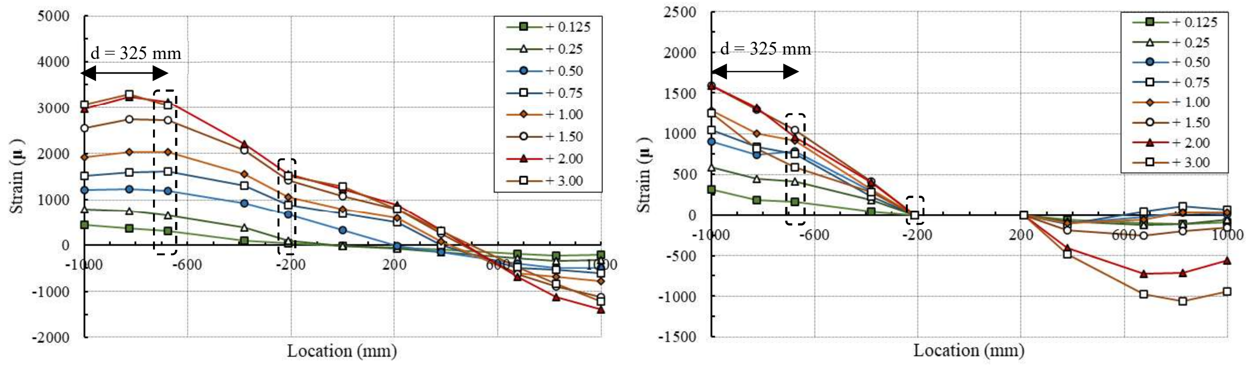

(a) First Layer Bar (b) Second Layer Bar

Fig. 5 – Longitudinal Bar Strain Distribution for N-5-3

The 1999 AIJ Guidelines bond strength τ_{bu2} is based on the side splitting bond failure, so τ_{bu2} increases as the ratio of clear bar spacing and ligament length for splitting increases. N-5-2, N-5-3, and N-5-4 have different clear bar spacing due to different number of second layer bars. But the results showed that the maximum bond strength of N-5-2, N-5-3, and N-5-4 was barely affected by the number of second layer bars. Alternatively, maximum bond stress of second layer bars can be evaluated using the lateral splitting mode proposed by Nishimura and Kawazu [3][4].

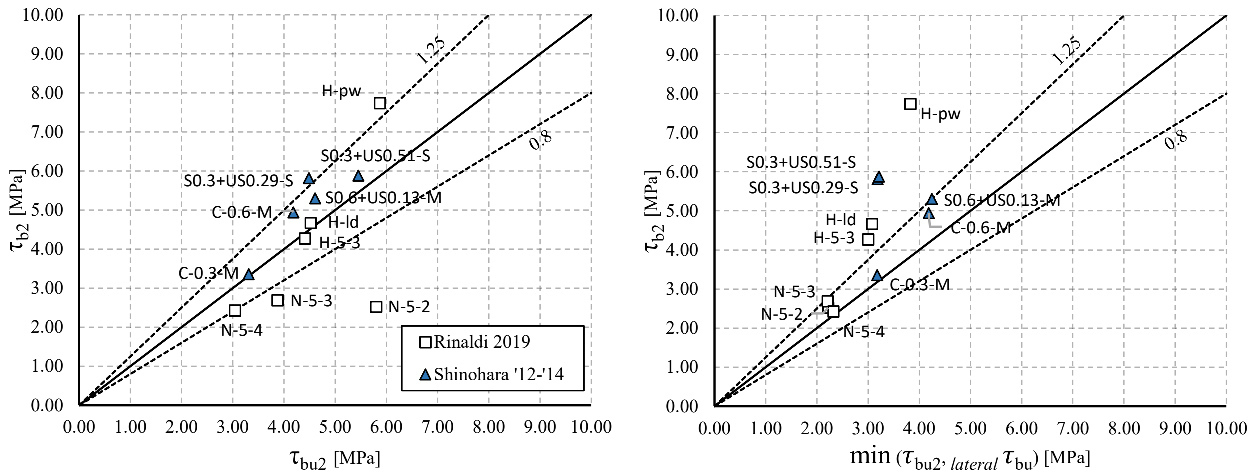

(a) Compared with τ_{bu2} (b) Compared with min (τ_{bu2}, ${}_{lateral}\tau_{bu}$)

Fig. 6 – Maximum Bond Stress of Second Layer Bars (τ_{b2})

Unlike τ_{bu2}, lateral split bond strength ${}_{lateral}\tau_{bu}$ is not affected by the number of second layer bars. The bond strength is affected by the number of bar layers and concrete cover given by the lateral splitting line shown in Fig. 1 (b). Figure 6 (b) compares the minimum of ${}_{lateral}\tau_{bu}$ and τ_{bu2} with the experimental value τ_{b2}. The lateral bond split strength ${}_{lateral}\tau_{bu}$ is lower than τ_{bu2} in most cases. N-5-2, N-5-3, and N-5-4 are in good agreement with the calculated values. The ratio of the experimental and calculated values $\tau_{b2}/\min(\tau_{bu2}, {}_{lateral}\tau_{bu})$ ranged from 1.04 to 2.02. The calculated bond strength was conservative compared to the experimental value with a mean average $\tau_{b2}/\min(\tau_{bu2}, {}_{lateral}\tau_{bu})$ of 1.31. Therefore, a minimum of τ_{bu2} and ${}_{lateral}\tau_{bu}$ should be used for estimating the bond strength of second layer bars.

4. Failure Modes

Table 2 shows some important factors in determining failure modes, such as the timing of maximum bond stress, crack occurrences, peak load, and reinforcement yielding. Lateral load (Q) and Drift Angle (R) relationship is shown in Fig. 7. Crack pattern at peak load is shown in Fig. 8.

Failure modes are classified into four categories, flexure failure, shear failure, bond failure, and a mixture of shear and bond failure. The failure mode is defined as flexure failure if the longitudinal reinforcement yield, and major flexural crack appears at the peak load, followed by crushing of concrete. None of the six specimens failed in flexure. Shear failure is indicated by major diagonal cracks, either or both of yielding of shear reinforcement, and/or concrete crushing of diagonal struts before or during the peak load. Bond failure is indicated by bond deterioration of longitudinal bars accompanied by bond splitting cracks along the longitudinal bars. If a combination of bond failure and shear failure indicators occurs, then the specimen is considered to fail in a mixture of shear and bond failure.

Figure 7(a) shows the load and drift angle relationship of N-5-2. Bond splitting cracks were observed at R=0.25%, followed by bond deterioration of two longitudinal bars at R=+1.08%. The other bars deteriorated at R=-0.96%, and +1.50%. Severe bond splitting cracks and spalling were observed at the peak load R=+2.02%, as shown in Fig. 7(a). These data suggest that bond deterioration decreased the force carried by the longitudinal bars in N-5-2. A similar damage process was observed in N-5-3 and N-5-4. Bond splitting cracks, followed by bond deterioration of longitudinal bars, were observed in both specimens. It was concluded that N-5-2, N-5-3, and N-5-4 failed in bond.

Bond and shear-type damages were observed in H-5-3. Bond cracks appeared at R=0.75%, and then followed by bond deterioration of two second layer bars at R=+1.34% and R=-1.39%. The other bars reached the maximum bond stress at or after the peak load. Major shear cracks and spalling were observed at the peak load. It was concluded that H-5-3 failed in a mixture of shear and bond. H-ld and H-pw followed the same damage process as H-5-3. Most of the bars reached the maximum bond stress at or after the peak load. Major shear cracks and spalling were observed as shown in Fig 8.

There were some general patterns found from the test. Figure 7 shows that the bond of external second layer bars deteriorated earlier than that of the interior bars. It appears that the bond of external bars were more vulnerable to bond failure. The first layer bars reached the maximum bond stress after the curtailed second layer bars. The occurrences of bond splitting cracks and bond deterioration delayed as the number of second layer bars and curtailment length increased as seen from N-5-2, N-5-3, and N-5-4. Bond deterioration delayed by increasing shear reinforcement, as seen from H-5-3 and H-pw. H-pw bond cracks appeared last among the other specimens at R=1.50%, since H-pw had the highest shear reinforcement ratio.

Table 2 – Experimental Values

No.		1	2	3	4	5	6
Specimen		**N-5-2**	**N-5-3**	**N-5-4**	**H-5-3**	**H-ld**	**H-pw**
Peak Load [kN]		353	415	460	429	448	625
Drift for Peak Load △ [%]		2.02	2.91	2.02	1.90	1.47	2.76
*Drift for τ_{b1} ■ [%]		1.08 B	2.02 B	2.01 B	2.01 A	2.00 A	-
*Drift for τ_{b2} ● [%]		1.08 B	1.43 B	1.51 B	1.34 B	1.47	2.76
Reinforcement Yield Drift [%]	Long.	-	-	-	-	-	1.96
	Transv.	-	-	-	-	3.00	-
Drift for First Bond Crack (%)		0.25	0.50	0.75	0.75	0.50	1.50
Drift for First Shear Crack (%)		0.125	0.25	0.125	0.125	0.25	0.25
Failure Mode		Bond	Bond	Bond	Shear and Bond	Shear and Bond	Shear and Bond

*Note: Letter “A” indicates maximum bond stress occurred after peak load.
Letter “B” indicates maximum bond stress occurred before peak load.
No letter indicates maximum bond stress occurred at peak load.

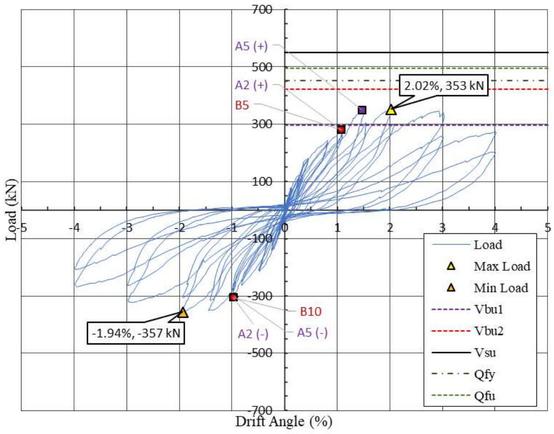

(a) No. 1 (N-5-2)

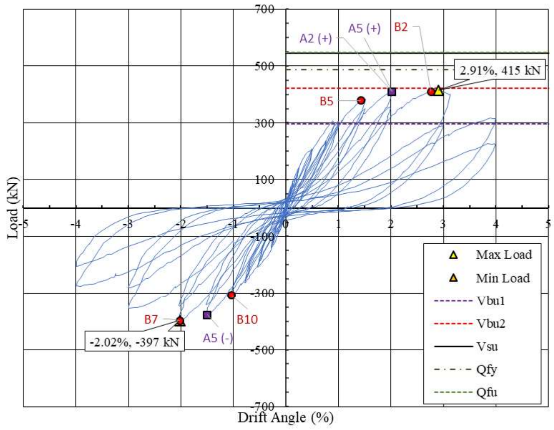

(b) No. 2 (N-5-3)

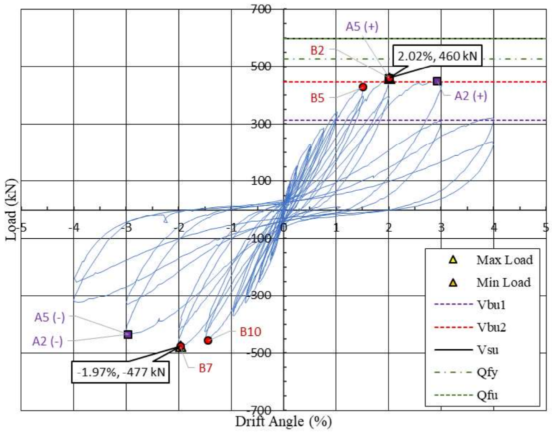

(c) No. 3 (N-5-4)

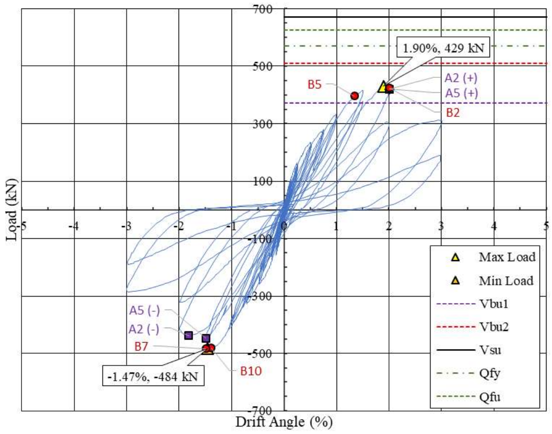

(d) No. 4 (H-5-3)

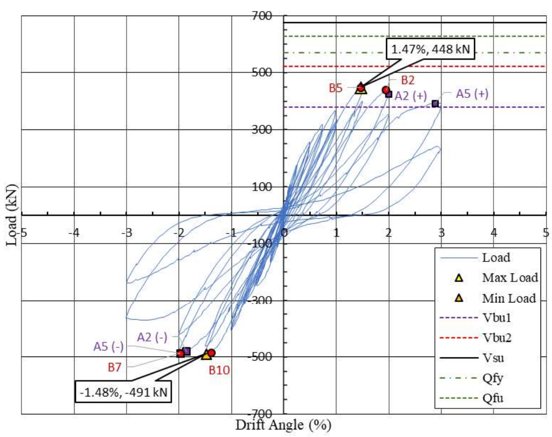

(e) No. 5 (H-ld)

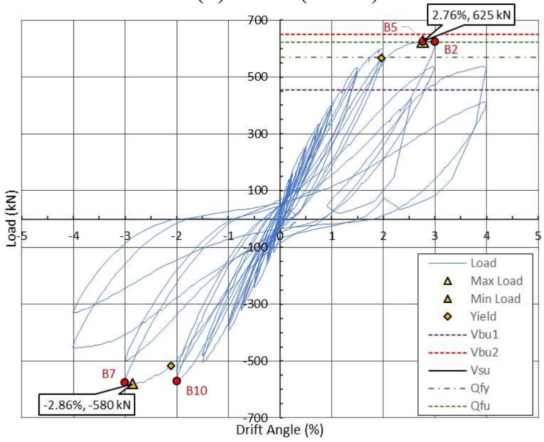

(f) No. 6 (H-pw)

Fig. 7 – Load (Q) and Drift Angle (R) Relationship

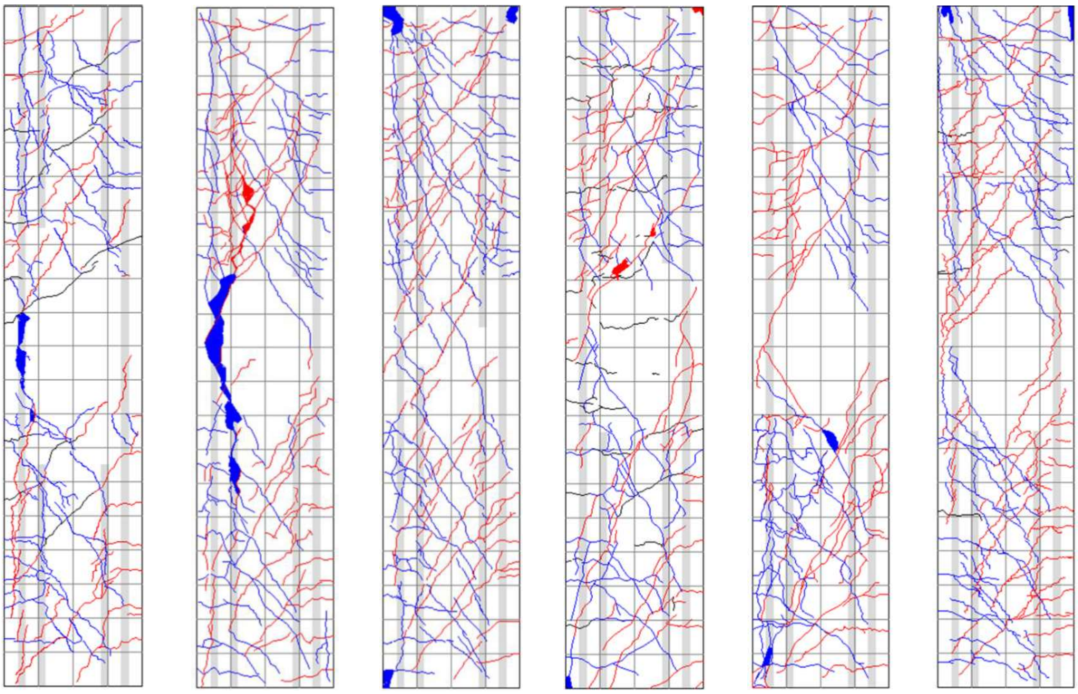

(a) N-5-2 (b) N-5-3 (c) N-5-4 (d) H-5-3 (e) H-ld (f) H-pw

Fig. 8 – Crack Pattern at Peak Load

5. Conclusions

An experimental study was conducted on six RC beams with curtailed second layer longitudinal reinforcement confined by 1275MPa class shear reinforcement. The maximum bond stress of second layer longitudinal bar is in good agreement with the calculated bond strength with a mean-average $\tau_{b2}/\min(\tau_{bu2}, {}_{lateral}\tau_{bu})$ of 1.31.

6. Acknowledgements

The authors express their gratitude to Neturen Co. Ltd. for their assistance and financial support. This study was undertaken at the Institute of Innovative Research and Collaborative Research Project of Materials and Structures Laboratory and the World Research Hub Initiative, Tokyo Institute of Technology.

7. References

[1] Architecture Institute of Japan (1999): *Design Guidelines for Earthquake Resistant Reinforced Concrete Buildings Based on Inelastic Displacement Concept.* (in Japanese)

[2] Architecture Institute of Japan (2018): *Standard for Structural Calculation of Reinforced Concrete Structures.* (in Japanese)

[3] Nishimura K, Kawazu M (2019): Experimental study on local bond failure of tension reinforcing bars embedded in concrete. *Journal of Structural and Construction Engineering*, Vol. 84 No. 762.1103-1113, AIJ, Japan. (in Japanese)

[4] Nishimura K, Onishi N, and Kawazu M (2020): Experimental Study on Bond Split Failure of Tension Reinforcing Bars Embedded in Concrete, *17th World Conference on Earthquake Engineering*, Sendai, Japan, #2c-0028.

[5] Shinohara Y, Murakami K (2014): Bond behaviors of second layer-cutoff bars reinforced by transverse bars having various configurations. *Journal of Structural and Construction Engineering*, AIJ, Japan. (in Japanese)

[6] Shinohara Y, Murakami K (2015): Effect of transverse reinforcement on bond splitting behaviors of RC beams with second layer-cutoff bars. *Journal of Structural and Construction Engineering*, AIJ, Japan. (in Japanese)

